Article

Research on 4N8 High-Purity Quartz Purification Technology Prepared Using Vein Quartz from Pakistan

Yutian Xie [1], Mei Xia [2,*], Xiaoyong Yang [2,*], Ibrar Khan [2] and Zhenhui Hou [2]

1   School of Physical Science, University of Science and Technology of China, Hefei 230026, China
2   State Key Laboratory of Lithospheric and Environmental Coevolution, University of Science and Technology of China (USTC), Hefei 230026, China; zhenhui@ustc.edu.cn (Z.H.)
*   Correspondence: xm851102@ustc.edu.cn (M.X.); xyyang@ustc.edu.cn (X.Y.)

Abstract: This study investigates the potential of two quartz vein ores from the Hunza District, Gilgit-Baltistan, Pakistan, as raw materials to obtain 4N8 high-purity quartz (HPQ) sand. Various quartz purification processes were examined, including ore calcination, water quenching, flotation, sand calcination, acid leaching, and chlorination roasting. Analytical techniques such as optical microscopy, Raman spectroscopy, and inductively coupled plasma spectroscopy were employed to analyze the microstructure, inclusion characteristics, and chemical composition of both the quartz raw ore and the processed quartz sand. Microscopic observation reveals that the PK-AML quartz raw ore has relatively high purity, the secondary fluid inclusions are arranged in a directional–linear manner or developed along crystal micro-cracks, and most intracrystalline regions exhibit low inclusion contents, while the PK-JTLT quartz raw ore contains a certain number of melt inclusions. The two processed quartz sand samples exhibit a smooth surface with extremely low fluid inclusion content. A comparative analysis of different purification processes shows that quartz sand calcination has a higher impurity removal rate than ore calcination. After crushing the raw ore into sand, the particles become finer with a larger specific surface area. Quartz sand calcination maximally exposes the inclusions and lattice impurity elements within the quartz, facilitating subsequent impurity removal through acid leaching. Following the processes of crushing, ultrasonic desliming, flotation, sand calcination, water quenching, acid leaching, and chlorination roasting, the SiO_2 content of PK-AML processed quartz sand is 99.998 wt.%, with only a small amount of Ti and Li remaining, and a total impurity element content of 20.83 $\mu g \cdot g^{-1}$. This meets the standard requirements for crucible preparation in industrial applications, making this vein quartz suitable for producing high-end HPQ products. In contrast, the overall purity of PK-JTLT quartz is lower, and the high contents of impurity elements such as Li, Al, and Ti are difficult to remove via purification experiments. The SiO_2 content of PK-JTLT processed quartz sand is 99.991 wt.%, which is applied to higher-quality glass products such as photovoltaic glass, electronic glass, and optical glass, thus presenting broad prospects for application.

Keywords: vein quartz; purification process; impurity elements; 4N8 high-purity quartz

1. Introduction

Quartz is commonly found in igneous, sedimentary, and metamorphic rocks and hydrothermal veins in nature, and it is a widely used mineral resource [1–4]. In recent years, the rapid development of industries such as solar energy, fiber optic communications, semiconductors, and microelectronics has led to increasing demand for high-purity quartz (HPQ), both in terms of quantity and quality. HPQ is an essential and irreplaceable functional material for these industries and is considered a scarce strategic resource globally [5–9]. HPQ is processed from natural quartz with minimal impurity levels such as crystal, granitic pegmatite quartz, and vein quartz [10–18]. Considering the quality of raw ore, detection methods, existing purification processes, and industry quality requirements,

Wang (2022) [19] established domestic quality standards for HPQ, defining quartz with SiO_2 content $\geq$99.9 wt.% as HPQ (Table 1).

Table 1. High-purity quartz quality standards commonly used in China.

Product Categories	SiO_2 Content	Total Amount of Impurity Elements
High-end products	$SiO_2 \geq$ 99.998 wt.% 4N8	Impurity content $\leq$ 20 $\mu g \cdot g^{-1}$, 4N8
Mid- to high-end products	$SiO_2 \geq$ 99.995 wt. % 4N5	Impurity content $\leq$ 50 $\mu g \cdot g^{-1}$, 4N5
Mid-range products	$SiO_2 \geq$ 99.99 wt.% 4N	Impurity content $\leq$ 100 $\mu g \cdot g^{-1}$, 4N
Low-end products	$SiO_2 \geq$ 99.9 wt.% 3N	Impurity content $\leq$ 1000 $\mu g \cdot g^{-1}$, 3N

With the gradual depletion of primary and secondary crystal resources, vein quartz is an ideal raw material ore to replace natural crystal as processing HPQ sand because of it has few gangue minerals, a coarse grain size, easy dissociation, and high SiO_2 content, so it meets the market requirements of the silicon industry and high-tech industry [20,21]. Researchers have conducted a lot of work on the processing of HPQ sand prepared from vein quartz, and it is believed that the impurities in vein quartz raw ore mainly exist in three forms: gangue minerals, inclusions, and lattice impurity elements [22–29]. Quartz purification techniques to remove these impurities usually include calcination, water quenching, crushing, ultrasonic desliming, screening, grinding, magnetic separation, flotation, acid leaching, and deep purification processes such as chlorination roasting, vacuum calcination, microwave calcination, microwave acid leaching, and hot press acid leaching. Among them, crushing, ultrasonic desliming, screening, grinding, magnetic separation, and flotation are physical purification methods, which can remove the surface impurities of quartz ore and gangue minerals associated with quartz. Calcination, water quenching, and acid leaching are chemical purification methods, which can remove the impurities and inclusions inside quartz, while deep purification experiments can further remove lattice impurity elements and inclusions less than 10 μm [10,30–41]. Lou et al. (2020) [40] carried out purification tests on three kinds of quartz sand samples via a chlorination roasting process. The results showed that Na, Fe, and K were significantly removed by roasting in a mixture of dry HCl gas, Cl_2, Cl_2, and HCl at 1000 °C for 2 h, and the purification effect of dry HCl gas was the best. Li et al. (2022) [18] combined microwave heating and ultrasonic-assisted acid leaching to remove Fe in quartz sand. When the quartz sand was treated by microwaves at 400 °C for 30 min, the micro-inclusions in the quartz sand burst and cracks formed around the quartz matrix, which is beneficial to the removal of impurities in the subsequent acid leaching. Subsequently, the residual Fe in the matrix was further removed under ultrasonic conditions. The content of Fe decreased from 285 $\mu g \cdot g^{-1}$ to 0.167 $\mu g \cdot g^{-1}$, and the removal rate was as high as 99.94%. Yang et al. (2024) [41] studied the kinetics of the hot-pressing leaching process of quartz from Lingqiu Mountain in Qichun, Hubei Province. It was found that at 210 °C, the mixed acid of HF, HCl, and HNO_3 was used to leach for 9 h at a liquid–solid ratio of 3:1. The removal rates of the main impurity elements, Al, Fe, Ca, and K, were high, and the SiO_2 content of the final product was 99.974%.

In this study, the gangue minerals, microstructure, and inclusion characteristics of two vein quartz samples were studied by optical microscopy, Raman spectroscopy, and scanning electron microscopy (SEM) using vein quartz from the Hunza Valley, Gilgit-Baltistan, Pakistan, as raw materials. Through different purification processes, the quality requirements of HPQ were evaluated after purification. By studying the mineralogical characteristics of vein quartz ore and its processing technology, this study provides a reference value for the selection of higher-quality HPQ raw ore and the optimization of related purification processes in the future.

2. Geological Background and Samples

2.1. Geological Background

Hunza Valley, situated west of the Baltoro region, offers excellent access to plutonic formations in the north and the Karakoram Metamorphic Complex (KMC). The Hunza

Plutonic Unit (HPU), a component of the Karakoram Batholith, comprises plutonic rocks extending along the valley and northern margin of the Hispar glacier (Figure 1). Previous investigations in the Hunza valley have indicated that the HPU of the Karakoram Batholith was thrust southward, overriding the sillimanite gneisses of the KMC [42–44]. The pre-collisional period of the Hunza Plutonic Unit (HPU) is punctuated by two post-collisional magmatic events [44]. Predominantly composed of quartz diorites and granodiorites, the HPU in the Hunza Valley region exhibits deformation resulting from collision-induced south-vergent thrusting to its southern extent. Geochronological analyses of these granodiorites have yielded a U-Pb age of 95 Ma [45] and an Rb-Sr age of 97 Ma [46].
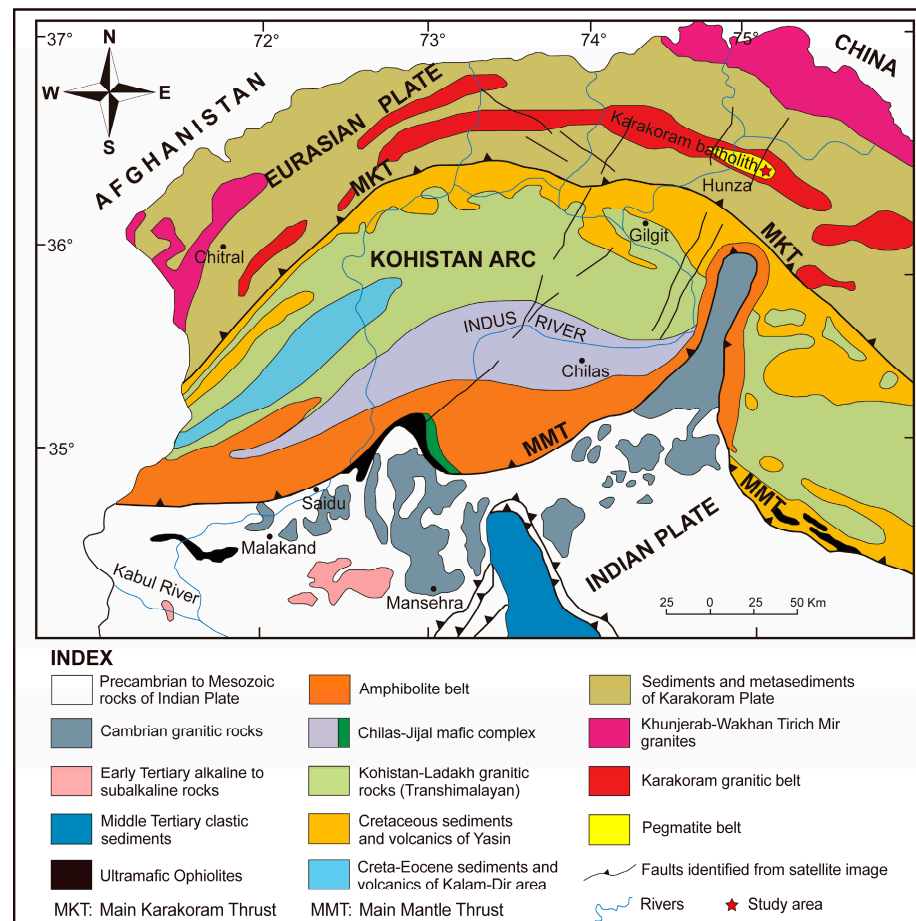

Figure 1. Geological map of the Kohistan (modified after Searle [45]). Sample locations are marked as red stars.

The most significant mineral and precious stone reserves in the Gilgit-Baltistan region of northern Pakistan are found in the Hunza Valley and the Haramosh Mountains. The base granite contains igneous rocks that are part of the Karakorum Metamorphic Complex (KMC), which are altered by the pegmatite bodies that pierce the metasediments. The pegmatite bodies in this area contain quartz, axinite, and epidote, which are found in the alpine clefts (Figure 1). The collision of the Indian and Eurasian plates, which resulted in the development of the Himalayan chain between 1 and 23 million years ago, is connected to this pegmatite region [47]. According to Malkani (2020) [48], pegmatites and suture zones are sources of quartz crystals, and well-formed, transparent quartz crystals are typically found in these pegmatites. These quartz veins from pegmatites exhibit spatial variability in their dimensions, ranging from several meters to less than one meter in width along the strike. Pakistan possesses numerous quartz vein deposits, which are utilized in various applications such as gemstones, dishware, optical devices, eyewear, chemical production, radio equipment, and electrical and radio apparatus frequency regulation.

In this study, two vein quartz samples (PK-AML and PK-JTLT) were collected from two different vein deposits in this area, to evaluate their potential as raw materials for the production of 4N8-HPQ.

2.2. Hand Specimen of Sample

The hand specimen photographs of PK-AML show that the quartz is milky white and opaque (Figure 2a,b), while the PK-JTLT quartz is white and semi-transparent (Figure 2c,d). Both quartz samples exhibit a massive structure, with uniform grain size, brittleness, a greasy luster, conchoidal fracture, and no cleavage surface (Figure 2a–d). Under the naked eye, a thin film of pale yellow and black-brown metallic oxides is observed on the local surface (Figure 2b,c), with no visible gangue minerals. Combined with the theoretical and previous research results, the characteristics of high-quality HPQ raw ore are that the mineral composition is mainly quartz, which has high transparency, a uniform particle size, and no gangue minerals visible to the naked eye [49,50]. Therefore, both vein quartz samples are of high quality, and the purification experiment can be conducted to prepare HPQ sand using these two samples.
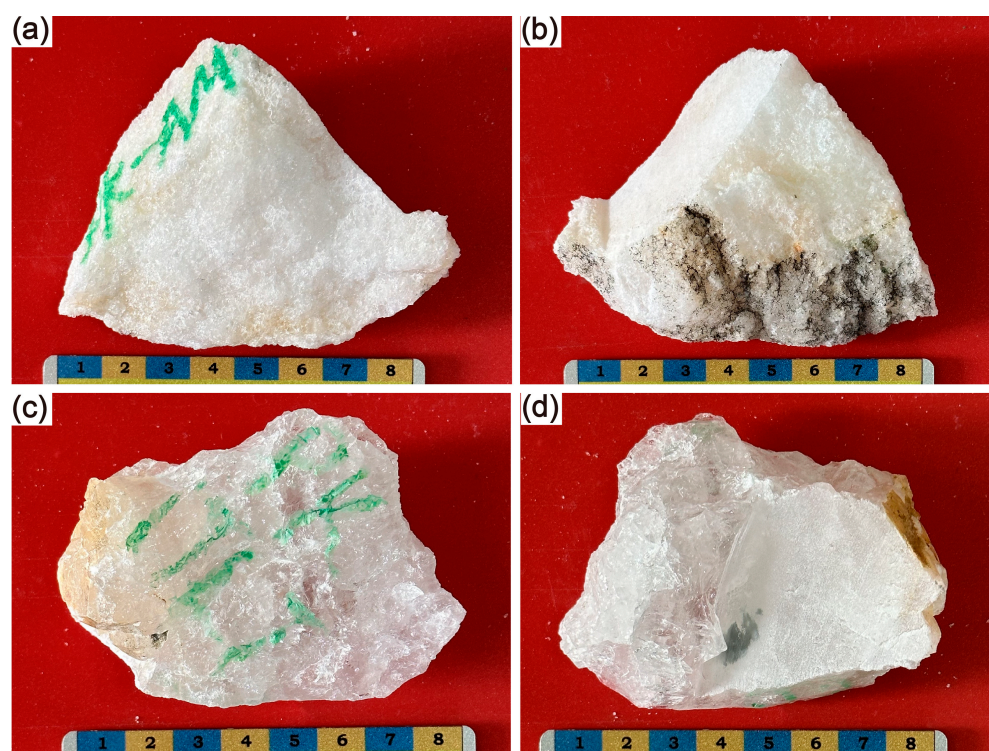

Figure 2. Hand specimens of vein quartz raw ore with a centimeter reference scale. (**a**,**b**) PK-AML, (**c**,**d**) PK-JTLT.

3. Purification Process

3.1. Experimental Reagents

In this study, all reagents used in the experiment were purchased from Sinopharm Chemical Reagent Co., Ltd., in Shanghai, China, including dodecylamine (CHN, AR), sodium dodecylbenzene sulfonate (CHNaO$_3$S, AR), hydrochloric acid (HCl, GR), nitric acid (HNO$_3$, GR), hydrofluoric acid (HF, GR), sulfuric acid (H$_2$SO$_4$, AR), sodium hydroxide (NaOH, AR), and manganese dioxide (MnO$_2$, AR). The resistivity of ultrapure deionized water used in the experiment was 18.25 MΩ·CM.

3.2. Experimental Procedures

In this purification experiment, three different experimental approaches were adopted. The specific experimental procedures are illustrated in Figure 3.
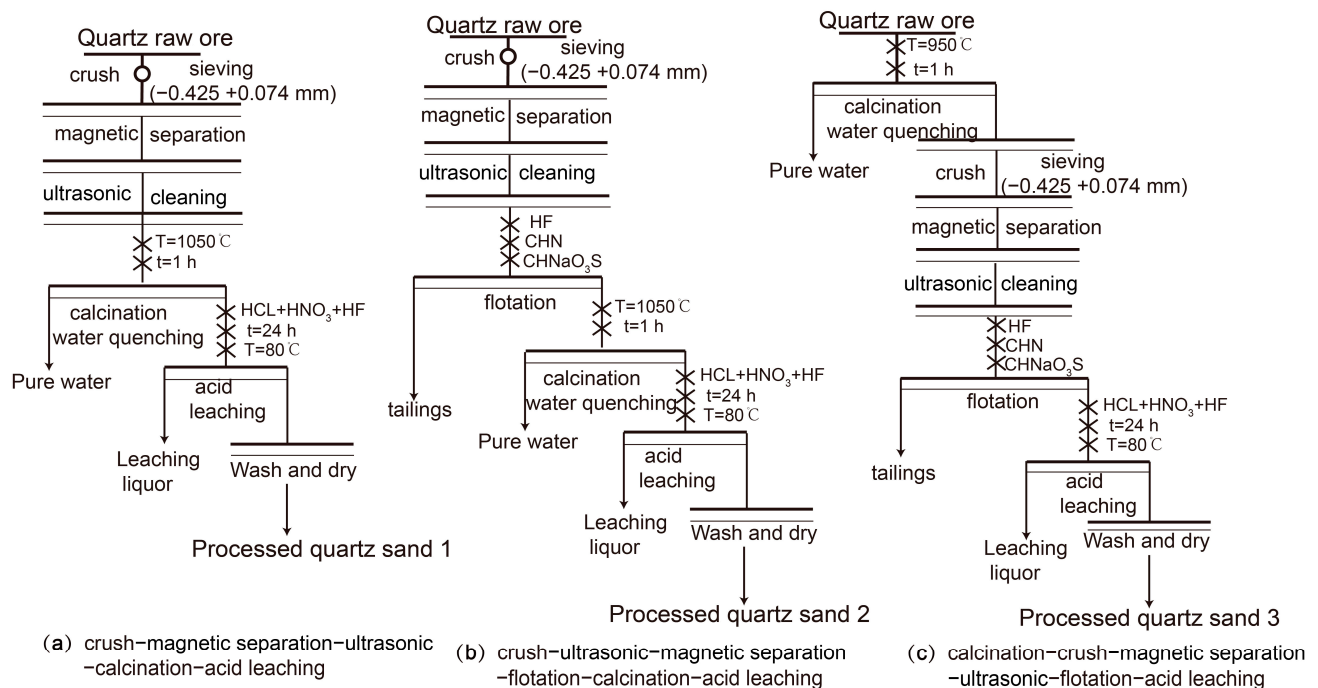
Figure 3. Flow chart of purification experiment. HF = hydrofluoric acid; HCl = hydrochloric acid; HNO_3 = nitric acid; CHN = dodecylamine; $CHNaO_3S$ = sodium dodecylbenzene sulfonate. $HF-HCl-HNO_3$ = 1:1:3.

Experimental procedure 1 is shown in Figure 3a. The purification experiments were as follows: crushing and screening, magnetic separation, ultrasonic desliming, calcination, water quenching, and acid leaching. A total of 1kg quartz raw ore was crushed into small millimeter-sized stones using a hammer. These crushed stones were then thoroughly washed and scrubbed with water to remove surface contaminants, including clay minerals and metal oxides, followed by air-drying. The crushed quartz stones were then crushed into quartz sand using a jaw crusher (PE−F100 × 125). The quartz sand was segregated into different fractions using standard nylon sieves, with particle sizes between −0.425 and 0.074 mm (40–200 mesh) being selected for ultrasonic scrubbing and desliming operations. This process involved a fixed scrub slurry concentration of 50% and ultrasonic cleaning three times, for 3 min each time, followed by two more rinses of quartz sand. The deslimed quartz sand was subjected to magnetic separation and then fed into a KSY-12-16A muffle furnace (KSl-1200X, KEJING, HeFei), and calcined at 1050 °C for 1 h with a calcination heating rate of 10 °C/min. The calcined quartz sand was then rapidly transferred into ultrapure water and subjected to ultrasonic cleaning three times before being dried. We accurately weighed 10.0 g calcined water-quenched quartz sand and placed it in a polyte-trafluoroethylene hydrothermal reaction vessel washed with ultrapure water. Subsequently, 10 g $HF-HCl-HNO_3$ mixed acid with a mass ratio of 1:1:3 was added to the reaction vessel, and acid leaching was carried out at 80 °C for 24 h. After acid leaching, the quartz sand was washed with ultrapure water under ultrasonic conditions until a neutral pH was reached, and then dried to obtain quartz sand 1.

Experimental procedure 2 is shown in Figure 3b. The purification experiments were as follows: crushing and screening, magnetic separation, ultrasonic desliming, flotation calcination, water quenching, and acid leaching. On the basis of experimental procedure 1, the ultrasonically deslimed quartz sand was subsequently added to the flotation experiment. In this experiment, an efficient and simple hydrofluoric acid flotation method was used. Hydrofluoric acid (HF) was used as the activator and an alkylamine surfactant was used as the cation collector.

An XFD-12 (0.5L) flotation machine was used in the flotation experiment. The stirring rate was 1500 rpm and the air flow rate was 0.25 m^3/h. In this work, the flotation temperature was controlled between 50 °C and 60 °C, and hydrofluoric acid was used to adjust and maintain the pH value of the slurry at 2–3 throughout the flotation process. First, 100 g deslimed quartz sand was added to a flotation cell containing 1.0 L ultrapure deionized water and stirred for 2 min. Subsequently, 2 mL dodecylamine (DDA) collector and 2 mL sodium dodecyl benzene sulfonate (SDBS) foaming agent were added to the flotation cell in turn, and the first flotation time was about 10 min. After the first flotation, half of the DDA and SDBS was used in the second scavenging flotation experiment. Finally, the quartz sand deposited at the bottom of the flotation cell was collected and dried to obtain quartz sand 2.

Experimental procedure 3 is shown in Figure 3c. The purification experiments were as follows: calcination, water quenching, crushing and screening, magnetic separation, ultrasonic desliming, flotation, and acid leaching. The cleaned quartz raw ore was placed into a KSY-12-16A muffle furnace (KSl-1200X, KEJING, HeFei) and subjected to calcination at 950 °C for 1 h. After calcination, the quartz blocks were promptly quenched by immersing them in ultrapure water. This process significantly reduced the hardness of the quartz ore. The ore was then crushed and screened, producing quartz sand with particle sizes ranging from −0.425 to 0.074 mm (40–200 mesh). This quartz sand underwent the same purification process as that described in experimental procedure 2, resulting in quartz sand 3.

3.3. Chlorination Roasting

The acid-leached quartz sand with the lowest impurity content in the three purification procedures was selected. A total of 8.0 g of acid-leached quartz sand was accurately weighed and roasted at 1050 °C in a Cl$_2$ atmosphere for 2 h; then, the processed quartz sand was obtained. Xia et al. (2024) [50] introduced the experimental steps of chlorination roasting in detail.

4. Analytical Methods

4.1. Optical Microscope Observation

Two quartz samples were prepared as double-polished thin sections for microscopic observation. The petrological characteristics of the quartz raw ore and the processed quartz sand, such as grain size, gangue minerals, fluid inclusions, and mineral micro-inclusions, were analyzed using a transmitted polarized light microscope (TPM, Nikon DS-RI2, Kyoto, Japan).

4.2. Scanning Electron Microscopy

The analysis of gangue minerals was carried out using a TESCAN MIRA3 scanning electron microscope (SEM) equipped with an EDAX GENESIS APEX Apollo System energy-dispersive spectrometer (EDS) at the State Key Laboratory of Lithospheric and Environmental Coevolution at the University of Science and Technology of China (USTC), Hefei, with working conditions of 15 kV and 15 nA for BSE imaging and EDS analysis.

4.3. Raman Spectroscopy

The Raman spectra of the fluid and melt inclusions in the quartz raw ore and the processed quartz sand were collected in situ using a Jobin-Yvon HORIBA LabRam HR Evolution confocal Raman micro-spectrometer (Kyoto, Japan) equipped with a 532 nm laser at the State Key Laboratory of Lithospheric and Environmental Coevolution in USTC, Hefei. The analytical conditions were as follows: a 1 μm beam diameter, a 200 μm slit width, a 100 μm confocal aperture, gratings with 600 grooves/mm, a 100× objective, 2× accumulations, and a 3 s acquisition time. The reliability of the data was ensured by testing monocrystalline silicon before testing the samples (520.7 cm^{-1} for a silicon metal standard).

4.4. Impurity Element Analysis

The determination of impurity element contents in quartz was carried out at the State Key Laboratory of Lithospheric and Environmental Coevolution in USTC, Hefei, using an Agilent 7700e quadrupole ICP-MS. Approximately 50 mg of sample was weighed and dissolved in a mixture of purified HNO_3 and HF. Simultaneously, the quartz standard material GBW07837 was also dissolved for comparison. Subsequently, the sample solutions underwent analysis using ICP-MS with an RF power of 1350 W and a nebulizer gas flow rate of 1.0 L/min. In order to eliminate the interference of polyatomic ion impurities, helium was introduced during the analysis at a flow rate of 3.5 mL/min as a collision gas. The standard correction curve solution for calculating the sample solution contents was prepared by standard solution comprising 13 elements, NCS181036, from NCS Testing Technology Co., Ltd. (Beijing, China). The concentrations of these elements in the mixture were set at 10 ppb, 40 ppb, 100 ppb, and 200 ppb, respectively.

5. Results and Discussion

5.1. Characteristics of Vein Quartz Ore

Whether natural quartz can be used as an HPQ raw material and what grade it reaches depend on the purifiability of the quartz, and the purifiability depends on the content and occurrence state of impurities in the quartz raw ore. The impurities in quartz raw ore are gangue minerals, inclusions, or lattice impurity elements depending on the difficulty of purification. The types of gangue minerals in different geological rocks are different. Vein quartz is usually associated with hematite, magnetite, feldspar, mica, etc. These mineral phases can also enter the quartz as mineral inclusions [51,52]. Fluid inclusions are the most common and abundant inclusions in quartz. They can be captured by quartz during the growth of quartz crystal to form primary fluid inclusions, and can also form secondary inclusions when the fluid penetrates along the micro-fractures of quartz and the quartz crystal heals. The most common component of fluid inclusions is water, but CO_2, CH_4, heavy hydrocarbons, and N_2 may also exist [1,21,51,52]. Quartz lattice impurity elements are introduced by point defects in quartz crystals. The elements Al^{3+}, B^{3+}, Fe^{3+}, Ge^{4+}, Ti^{4+}, and P^{5+} will substitute part of Si^{4+} in the quartz lattice and form lattice impurities. Furthermore, the impurity ions H^+, Li^+, Na^+, K^+, and Fe^{2+} enter the interstitial space to maintain the charge balance [1,21,51]. Generally, the common gangue minerals of quartz can be removed by crushing, magnetic separation, and flotation experiments. Most of the fluid inclusions larger than 10 μm can also be removed by high-temperature calcination and acid leaching experiments. However, the lattice impurity elements and inclusions less than 10 μm in quartz are difficult to completely remove using existing purification processes [16,20,50], which will directly affect the quality and industrial use of quartz resources.

5.1.1. Microstructure Characteristics

The quartz ores were ground into thickened polished thin sections (100 μm), and the structure, gangue minerals, and inclusion characteristics were studied thoroughly and systematically. Figure 4 shows the microtexture of PK-AML and PK-JTLT vein quartz samples observed under single polarization. The PK-AML quartz grains are intact and have good crystallinity, and the PK-JTLT grains are larger and have a block structure (Figure 4a–c). The PK-AML quartz is xenomorphic granular with a medium–coarse granular metacrystalline structure. The grain size is about 0.2–2 mm, and the grain boundary is relatively clear, and mostly linear and jagged (Figure 4a,b). The PK-JTLT quartz has a large grain size, blurred grain boundaries, and a small number of cracks in the crystal (Figure 4c). No gangue minerals were found by SEM observation, and the quartz content of the two samples was high.
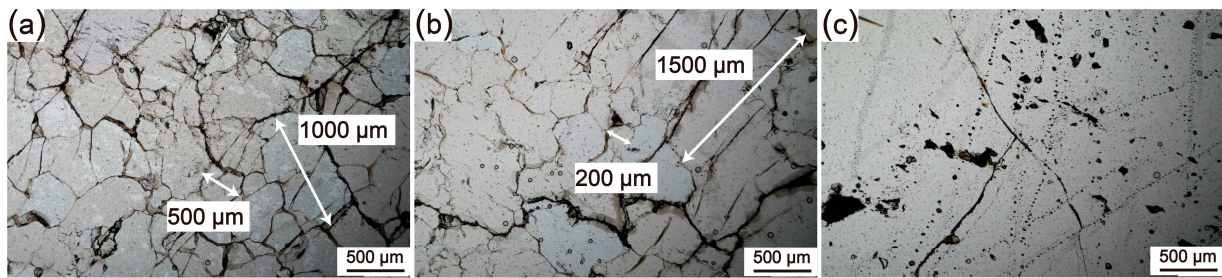
Figure 4. Microphotographs (plain polarized light) of vein quartz raw ore. (**a**,**b**) PK-AML vein quartz. (**c**) PK-JTLT vein quartz.

5.1.2. Inclusion Characteristics

Fluid inclusions, which are often found in vein quartz, are mainly primary and secondary fluid inclusions. The quality of HPQ raw ore materials is significantly affected by the quantity, size, distribution, and composition of these inclusions. Secondary fluid inclusions are the predominant type seen in high-quality vein quartz, and are less numerous, greater in size, and small in distribution range. These inclusions, especially those larger than 10 µm, are easy to burst and remove under high temperature and high pressure [51]. The fluid inclusions in the PK-AML vein quartz samples are mainly distributed in a band-like or clustered arrangement along the micro-cracks, predominantly as secondary inclusions, and the size is generally less than 5 µm (Figure 5a–c). These inclusions exhibit both gas–liquid and pure liquid phases, characterized by elongated, elliptical, and irregular forms (Figure 5d,e). At the same time, some areas of the crystal are relatively clean, with almost no inclusions (Figure 5f). The PK-JTLT vein quartz has few fractures and primary fluid inclusions, and the total number of inclusions is relatively low. A large number of directional–linear secondary fluid inclusions are distributed in the crystal, mainly elliptical, and the size of the inclusions is usually less than 10 µm (Figure 5g–i). At the same time, the crystal also contains a certain number of approximately circular melt inclusions, and the largest is greater than 20 µmm (Figure 5g,h,j–l). The Raman spectroscopy test of inclusions larger than 5 µm in two quartz samples shows that the gas–liquid inclusions have peaks at 1280 cm^{-1} and 1380 cm^{-1}, which are the characteristic peaks of CO_2, and peaks at 1610 cm^{-1}, 2900 cm^{-1}, and 3060 cm^{-1}, which are the characteristic peaks of H_2O (Figure 6). The Raman spectroscopy result of pure liquid inclusions in the PK-AML sample shows that it is H_2O. The melt inclusions in PK-JTLT vein quartz are usually not homogenous and can include vapor and solid phases, and their composition is rarely identified using Raman spectroscopy. In general, PK-AML vein quartz samples mainly contain pure liquid and gas–liquid secondary fluid inclusions, which are arranged in a directional–linear manner or developed along crystal micro-cracks, and are easily removed by explosions during quartz sand making, calcination, and water quenching. In addition, the content of inclusions in most areas of the crystal is very low, or even relatively absent. Based on the characteristics of the inclusions, the PK-AML vein quartz is considered to be of very high quality as a raw material [50,51]. However, the PK-JTLT vein quartz contains a certain number of melt inclusions, which are significantly smaller than quartz sand and are easily wrapped by quartz sand. Therefore, the existence of these melt inclusions increases the difficulty of purification.
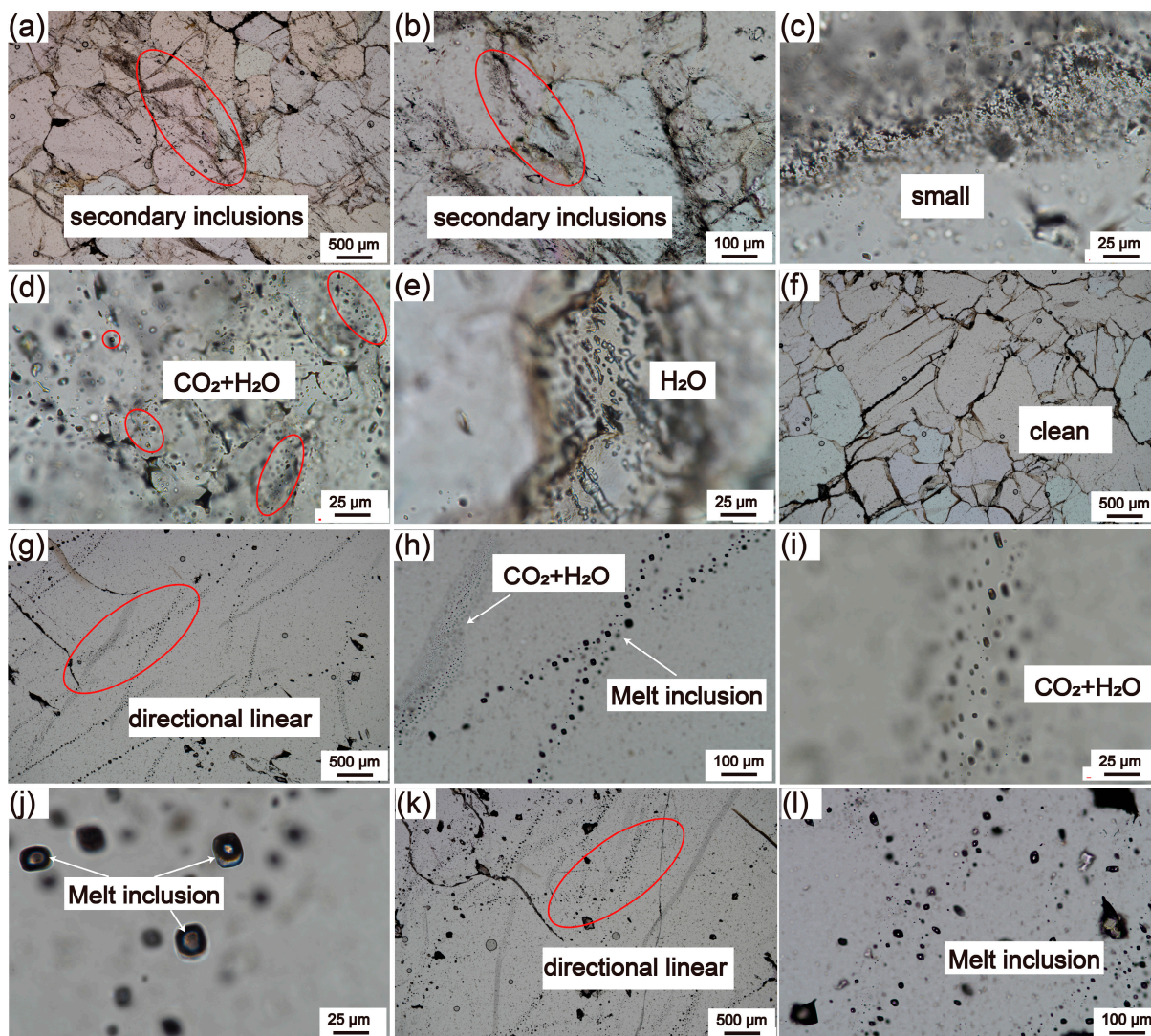
Figure 5. Microphotographs (TPM) of inclusions in the vein quartz raw ore. (**a**–**e**) PK-AML with a certain number of secondary fluid inclusions. (**f**) PK-AML with a relatively clean intracrystalline area. (**g**–**l**) PK-JTLT with a number amount of directional–linear secondary fluid inclusions and melt inclusions.

5.1.3. Chemical Composition

The quality and purification potential of quartz are influenced by the SiO_2 content and the presence of impurities in the raw ore, which ultimately determine the economic value and possible applications of the quartz raw material. The ICP-MS compositional analysis of the quartz raw ore (Table 2) revealed that the SiO_2 content of the PK-AML quartz raw ore was 99.990%, with the main impurity elements including Na (9.59 $\mu g \cdot g^{-1}$), Mg (11.10 $\mu g \cdot g^{-1}$), Al (47.37 $\mu g \cdot g^{-1}$), Ca (20.39 $\mu g \cdot g^{-1}$), Ti (8.41 $\mu g \cdot g^{-1}$), and Fe (4.55 $\mu g \cdot g^{-1}$), and the total impurity element content was 103.87 $\mu g \cdot g^{-1}$. In comparison, the SiO_2 content of the PK-JTLT quartz raw ore was 99.972%, with the main impurity elements including Li (39.35 $\mu g \cdot g^{-1}$), Na (4.94 $\mu g \cdot g^{-1}$), Mg (5.22 $\mu g \cdot g^{-1}$), Al (175.07 $\mu g \cdot g^{-1}$), K (27.44 $\mu g \cdot g^{-1}$), Ca (3.85 $\mu g \cdot g^{-1}$), Ti (4.13 $\mu g \cdot g^{-1}$), and Fe (17.58 $\mu g \cdot g^{-1}$), and the total impurity element content was 278.95 $\mu g \cdot g^{-1}$. The relatively high levels of the impurity elements Al and Ti in the PK-AML quartz ore and Al and Li in the PK-JTLT quartz ore are primarily attributed to lattice impurities, undetected gangue minerals, and melt inclusions, while Na, Mg, K, and Ca may be mainly introduced through various inclusions or undetected gangue minerals. The abnormally high levels of the impurity elements Al and Li in the PK-JTLT quartz raw

ore present significant challenges for purification [7,50]. Additionally, the high levels of the impurity element Fe in both samples may be introduced by the thin films of light yellow and dark brown iron oxides on the quartz surface.
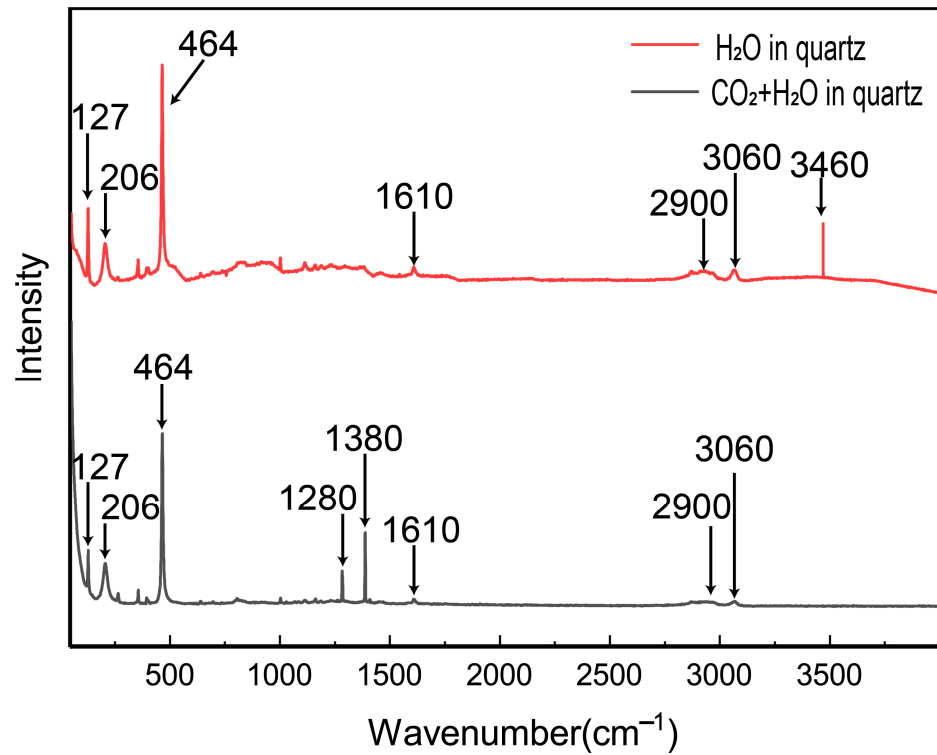

Figure 6. Raman spectra of fluid inclusions in PK-AML and PK-JTLT vein quartz.

Table 2. Impurity element contents ($\mu g \cdot g^{-1}$) in quartz raw ore and processed quartz sand determined by solution ICP-MS analysis.

	PK-AML						PK-JTLT			
Elements	Raw Ore	Quartz Sand 1	Quartz Sand 2	Quartz Sand 3	Chlorinated Quartz Sand	IOTA-STD	Raw Ore	Quartz Sand 1	Quartz Sand 2	Quartz Sand 3
Li	0.44	0.43	0.54	0.92	0.51	0.90	39.35	33.37	29.96	32.73
B	bdl	bdl	0.24	0.20	0.28	0.08	0.09	bdl	0.26	0.73
Na	9.59	6.36	3.60	5.51	0.59	0.90	4.94	3.03	2.44	5.08
Mg	11.10	0.81	0.09	0.71	0.06	<0.05	5.22	0.45	0.06	1.53
Al	47.37	16.50	14.19	18.29	14.16	16.20	175.07	176.86	54.66	115.59
K	bdl	1.21	0.02	0.11	0.05	0.60	27.44	bdl	0.03	0.09
Ca	20.39	4.42	0.53	5.41	0.45	0.50	3.85	bdl	0.17	1.78
Ti	8.41	4.66	4.29	4.17	4.15	1.10	4.13	4.32	4.00	4.32
Cr	0.19	0.04	0.01	0.08	0.05	<0.05	0.54	0.01	0.04	0.02
Mn	1.62	0.06	0.01	0.06	0.02	<0.05	0.45	0.07	0.03	0.05
Fe	4.55	1.77	0.27	0.56	0.44	0.23	17.58	0.50	0.38	0.84
Ni	0.16	0.01	0.02	0.08	0.06	<0.05	0.20	bdl	0.04	0.03
Cu	0.05	0.08	0.05	0.06	0.01	<0.05	0.08	bdl	0.04	0.04
sum	103.87	36.35	23.86	36.16	20.83	<19.66	278.95	218.59	92.11	162.83
SiO_2 (wt.%)	99.990	99.996	99.998	99.996	99.998	>99.998	99.972	99.978	99.991	99.984

IOTA-STD is the main product of United States Unimin Corporation. bdl: below the detection line. SiO_2 (wt.%) = $(1 - \Sigma/1{,}000{,}000) \times 100$. Quartz sand 1: crushing and screening, ultrasonic desliming, calcined water quenching, and acid leaching. Quartz sand 2: crushing and screening, ultrasonic desliming, flotation, calcined water quenching, and acid leaching. Quartz sand 3: Calcined and water quenching, crushing and screening, ultrasonic desliming, flotation, and acid leaching. Chlorinated quartz sand: quartz sand 2 under chlorination roasting.

5.2. Purification Process of Quartz

The process of purifying quartz primarily involves three main stages: pre-treatment, physical purification, and chemical purification. Each purification method corresponds to different types of impurities, and the goal of purification can be effectively achieved by organically combining different purification methods according to the types of impurities in quartz ores [53].

5.2.1. Pre-Treatment of Quartz Sand

Pre-treatment encompasses various steps, such as crushing, washing, de-silting, screening, and grinding. During the mining of quartz ore, a large number of clay minerals, cements, and metal oxide films are adhered to the surface of the quartz, which contain high contents of Fe and Al elements. As the quartz particles are ground to the desired industrial granularity of $-0.425 + 0.074$ mm (40–200 mesh), the surface content of impurities such as Fe and Al increases [30]. These impurities can be effectively reduced through scrubbing and desliming. Research by Zhao et al. (2004) [31] indicates that metal impurities on the surface of quartz particles are easily removed into the liquid phase under the action of ultrasonic waves. In this experiment, these surface impurities of quartz were removed by adding ultrasound.

5.2.2. Physical Purification of Quartz Sand

Physical purification mainly involves processes like magnetic separation, flotation, etc. Magnetic separation is a purification process employed to remove magnetic impurities in quartz ore through the action of a magnetic field. This process can not only remove magnetic impurities in quartz, but also remove magnetic inclusions. According to the magnetic strength, magnetic separation can be divided into weak magnetic separation and strong magnetic separation. Weak magnetic separation can remove impurities with strong magnetic properties, such as magnetite. Strong magnetic separation can remove impurity minerals with weak magnetism, such as hematite, ilmenite, biotite, etc. [10,54]. Since quartz ore is easily polluted by the crusher during the crushing process, quartz sand contains a large number of iron chips that need to be removed by magnetic separation. At the same time, quartz ore itself may also contain undiscovered magnetic minerals, so magnetic separation is necessary.

Flotation is a purification process that uses different crystal structures and surface properties of quartz and impurity minerals, especially surface hydrophobicity, and uses various collectors or surface activators to adjust the surface characteristics of mineral particles to separate impurities from quartz. During the flotation process, hydrophobic particles can attach to bubbles and then rise to the top of the floatation cell, while hydrophilic particles sink to the bottom of the cell [35]. This method exploits differences in surface hydrophobicity among minerals, and quartz sand with SiO_2 content of 99.3%~99.9% can be obtained [32–37]. The purpose of flotation is to further remove surface impurities such as metal oxide films, cements, and clay minerals on the surface of quartz ore and gangue minerals associated with quartz. Since no gangue minerals were found in both quartz samples used in this study, flotation experiments were theoretically not required. However, due to the small SEM detection sample, gangue minerals in the quartz ore may not have been found. In order to further remove these undiscovered gangue minerals and the surface impurities of quartz sand, a flotation experiment may be necessary. The flotation separation of quartz, feldspar, and mica is the most common flotation application in quartz sand purification. PK-AML and PK-JTLT quartz ores also contain a certain amount of the impurity elements Al, Na, K, and Ca that may occur in undetected feldspar and mica, so this experiment adopts the efficient and convenient fluorine acid flotation method, under the condition of pH 2–3, with HF as an activator and an alkylamine surfactant as a cationic collector for the flotation experiment [55–58].

5.2.3. Chemical Purification of Quartz Sand

Chemical purification primarily consists of high-temperature calcination followed by quenching and acid leaching. Quartz will undergo a phase transition during high-temperature calcination, accompanied by a crystal structure and volume change. In this process, the inclusions inside the quartz will undergo volume expansion, or even burst, resulting in micro-cracks in the adjacent matrix. The high-temperature quartz sand is directly quenched and cooled, and the high thermal stress gradient during the rapid cooling of quenching is used to further promote the formation and expansion of micro-cracks, so that the impurity phase originally existing in the quartz particles is revealed [24,38]. In industry, quartz blocks larger than 5 cm are usually calcined and quenched at about 900 °C. However, after crushing the raw ore into sand, the particles become finer with a larger specific surface area. Quartz sand calcination can expose the inclusions and lattice impurity elements in quartz to a greater extent [38,59]. Zhao et al. (2005) [60] studied the effect of high-temperature calcination on the surface of quartz sand and found that quartz ore can easily adsorb Na, K, Ca, Fe, Al, and Mg ions in the surrounding environment when it is broken into sand, which are mainly adsorbed on the surface of sand particles in the form of nano-scale oxides or hydroxides. These impurity elements are not easy to remove by pretreatment. When the quartz sand is calcined at a high temperature, the surface structure is reorganized, which reduces the adsorption capacity of the quartz sand surface onto the impurity phase particles, thereby purifying the quartz sand surface. Zuo et al. (2022) [38] studied the deep purification process of Fengyang quartz sand and proved that quartz ore is broken into smaller quartz sand for calcination and quenching treatment, which can greatly increase the escape ability of impurities during calcination and the cooling rate and thermal stress during quenching, and promote the generation of micro-cracks in quartz particles. Therefore, this experiment was carried out using two techniques: quartz ore calcination and sand calcination.

The calcined quartz sand was then subjected to acid leaching treatment. According to different acid leaching conditions, it was divided into atmospheric-pressure acid leaching and hot press acid leaching. In recent years, the hot press acid leaching method has become an important means of vein quartz purification because it can effectively improve leaching rate and leaching efficiency under high-temperature and high-pressure conditions [15,24,41]. When quartz sand is subjected to hot press acid leaching, HF in the leaching agent has a strong corrosive effect on the quartz, resulting in a large number of corrosion pits on the surface of the quartz, and further widening and deepening the cracks generated during the calcination–water quenching process. The leaching solution can diffuse into the quartz lattice and react with the impurities inside the crystal, so that the inclusions wrapped in the quartz and some lattice impurity elements can be dissolved and removed [24,29,38,39]. Zhong (2015) [24] conducted a study on the hot press acid leaching of quartz sand and demonstrated that a combination of mixed acids can produce a synergistic effect, resulting in more efficient impurity removal when using HCl–HF–HNO$_3$ with a mass ratio of 3:1:1. Liu (2017) [59] studied the calcination–acid leaching process of quartz sand. The results showed that the quartz sand was calcined at 1000 °C for 1 h, and then leached in a 90 °C water bath mixed with acid for 6 h. The impurity elements Al and Fe in quartz had the best removal effect. The removal rate of Al was 96.3%, and the removal rate of Fe was 85%. Combined with the previous research results and the actual situation of industrial production, the experimental conditions of calcination–hot press acid leaching were as follows: quartz sand was calcined at 1050 °C for 1 h and then quenched in water, and then placed in a HCl–HF–HNO$_3$ mixed acid system (with a mass ratio of 3:1:1 and a liquid/solid ratio of 1:1), with acid leaching at 80 °C for 24 h.

5.3. Characteristics of Processed Quartz Sand

5.3.1. Microscopic Characteristics

The quartz ore underwent three purification processes to produce pure white quartz sand (Figure 7a,g). TPM observation shows that the surface morphologies of PK-AML and

PK-JTLT acid-leached quartz sand are very similar, with numerous cracks appearing on the particle surface, whether it was under raw ore calcination or quartz sand calcination (Figure 7b,d,h,j). Compared with the raw ore calcination, the acid-leached quartz sand after sand calcination has more enlarged and deepened micro-cracks with approximately parallel arrangement (Figure 7e,k), which can expose the inclusions and lattice impurity elements in quartz to a greater extent [39]. At the same time, a large number of particles without fluid inclusions can be seen inside the PK-AML quartz sand, and only a small number of fluid inclusions can be observed inside the particles, which are composed of H_2O and CO_2 (Figure 7b–f). The content of fluid inclusions in the PK-JTLT quartz sand is even lower, and almost no quartz sand particles with residual fluid inclusions are observed, but a certain number of melt inclusions remain in some quartz sand particles (Figure 7h–l). Overall, the PK-AML and PK-JTLT quartz sands are pure white and clean, with high transparency and low inclusion content, and are therefore deemed to be of high quality.
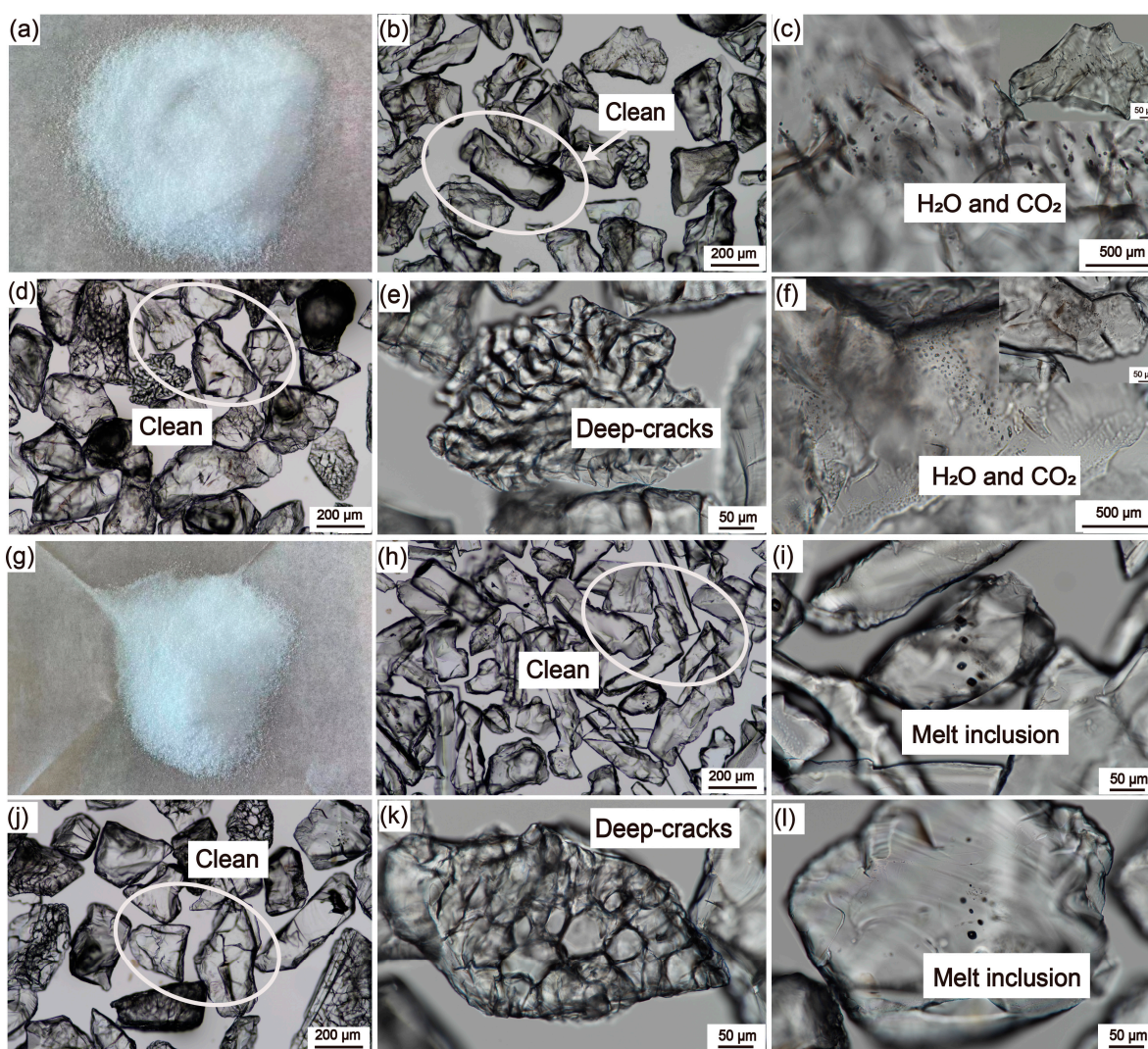

Figure 7. Microphotographs (TPM) of processed quartz sand. (**a**) Hand specimen of PK-AML processed quartz sand. (**b**,**c**) PK-AML acid-leached quartz sand after raw ore calcination. (**d**–**f**) PK-AML acid-leached quartz sand after sand calcination. (**g**) Hand specimen of PK-JTLT processed quartz sand. (**h**,**i**) PK-JTLT acid-leached quartz sand after raw ore calcination. (**j**–**l**) PK-JTLT acid-leached quartz sand after sand calcination.

5.3.2. Chemical Composition

Following pretreatment, physical purification, and chemical purification, the total content of impurity elements in the acid-leached quartz sand was significantly reduced. The ICP-MS analysis results in Table 2 indicate that the residual impurity elements in the PK-AML acid-leached quartz sand were mainly Na, Al, Ca, and Ti, and the total content of impurity elements in quartz sands 1, 2, and 3 were 36.35 $\mu g \cdot g^{-1}$, 23.86 $\mu g \cdot g^{-1}$, and 36.16 $\mu g \cdot g^{-1}$, with SiO_2 contents of 99.996 wt.%, 99.998 wt.%, and 99.996 wt.%, respectively. After flotation, the residues of the impurity elements Al, Na, and Ca in the calcined quartz sand were significantly reduced compared to the non-flotation quartz sand, decreasing to 14.19 $\mu g \cdot g^{-1}$, 3.6 $\mu g \cdot g^{-1}$, and 0.53 $\mu g \cdot g^{-1}$, respectively, whereas, K, Mg, and Fe also decreased to a certain extent. Compared to sand calcination, raw ore calcination resulted in higher residual impurity elements of Na (5.51 $\mu g \cdot g^{-1}$) and Ca (5.41 $\mu g \cdot g^{-1}$) in the acid-leached sand, likely due to more inclusions remaining in the ore-calcined sand. The three purification methods are less effective at removing the impurity element Ti (4.29 $\mu g \cdot g^{-1}$) from the quartz. However, the overall level of Ti in the quartz raw ore is not high, suggesting that this element is primarily a lattice impurity.

The PK-JTLT acid-leached quartz sand exhibited a high content of the impurity elements Al and Li, and a small amount of Na and Ti. The total impurity elements of quartz sands 1, 2, and 3 were 218.59 $\mu g \cdot g^{-1}$, 92.11 $\mu g \cdot g^{-1}$, and 162.83 $\mu g \cdot g^{-1}$, and the SiO_2 contents were 99.978 wt.%, 99.991 wt.%, and 99.984 wt.%, respectively. After flotation, the Al content, which is a major impurity element, decreased significantly in both the sand-calcined (Al: 54.66 $\mu g \cdot g^{-1}$) and ore-calcined (Al: 115.59 $\mu g \cdot g^{-1}$) samples, suggesting that the PK-JTLT quartz raw ore may contain an undiscovered high-Al impurity, making a flotation experiment necessary. However, regardless of whether the purification is conducted with sand calcination or ore calcination, the residual impurity elements Al (54.66 $\mu g \cdot g^{-1}$ and 115.59 $\mu g \cdot g^{-1}$), Li (29.96 $\mu g \cdot g^{-1}$ and 32.73 $\mu g \cdot g^{-1}$), and Ti (4.00 $\mu g \cdot g^{-1}$ and 4.32 $\mu g \cdot g^{-1}$) in the acid-leached sand are still high, especially the Al and Li elements. These impurity elements may have two occurrence states: one is the lattice impurity element, and the other is the residual melt inclusion in the quartz sand. Both Ti and Li are medium incompatible elements, which tend to be enriched in silicate melts during mineral crystallization, and the content of Al in melt inclusions is also relatively high. As a result, the overall purity of PK-JTLT quartz is relatively low, and the high content of the impurity elements Li, Al, and Ti is difficult to remove via purification experiments.

The different purification processes of these two vein quartz samples prove that a flotation experiment is essential for vein quartz, as it helps to remove impurities like surface impurities and undiscovered gangue minerals in the samples. Simultaneously, crushing quartz raw ore into sand creates finer particles with a larger surface area. Quartz sand calcination can more extensively expose the inclusions and lattice impurity elements within the quartz, making it more effective for subsequent acid leaching to remove impurities [24,29,38,39].

5.4. Deep Purification and Economic Assessment with Vein Quartz

The overall purity of PK-AML quartz is high, with the SiO_2 content of acid-leached quartz sand 2 as high as 99.998 wt.% (4N8). There are still a certain number of lattice impurity elements such as Na, Al, and Ti in the acid-leached quartz sand; the impurity element Na especially does not meet the standard of ultra-HPQ sand. In order to further remove these impurities, a chlorination roasting experiment was carried out on the PK-AML acid-leached quartz sand. Chlorination roasting refers to the chlorination reaction of metal impurity elements in quartz sand with a chlorination agent under certain conditions, generating gaseous chlorides and volatilizing them to achieve effective separation of metal impurity elements [25,28,40,61,62]. The ICP-MS analysis in Table 2 revealed that the total impurity elements in the PK-AML acid-leached quartz sand 2 decreased to 20.83 $\mu g \cdot g^{-1}$ after the chlorination roasting process. Chlorination roasting shows limited effectiveness in removing the lattice impurity elements Al and Ti from quartz. However, the impurity

element Na shows a significant reduction from 3.60 $\mu g \cdot g^{-1}$ in acid-leached quartz to 0.59 $\mu g \cdot g^{-1}$, indicating a notable purification effect. The quality standard of IOTA-STD (standard material) of Unimin is shown in Table 2: the content of SiO_2 is 99.998%, with a total impurity element content of 19.66 $\mu g \cdot g^{-1}$. The contents of the impurity elements Al and Ti are 16.2 $\mu g \cdot g^{-1}$ and 1.1 $\mu g \cdot g^{-1}$, respectively, and the content of other impurity elements is less than 1 $\mu g \cdot g^{-1}$ [19]. Compared with Unimin standard sand, the content of the impurity element Al in PK-AML processed quartz sand is lower than that in standard sand, and the other impurity elements are lower than 1 $\mu g \cdot g^{-1}$. Only the content of the impurity element Ti is significantly higher than that i standard sand (Table 2, Figure 8).
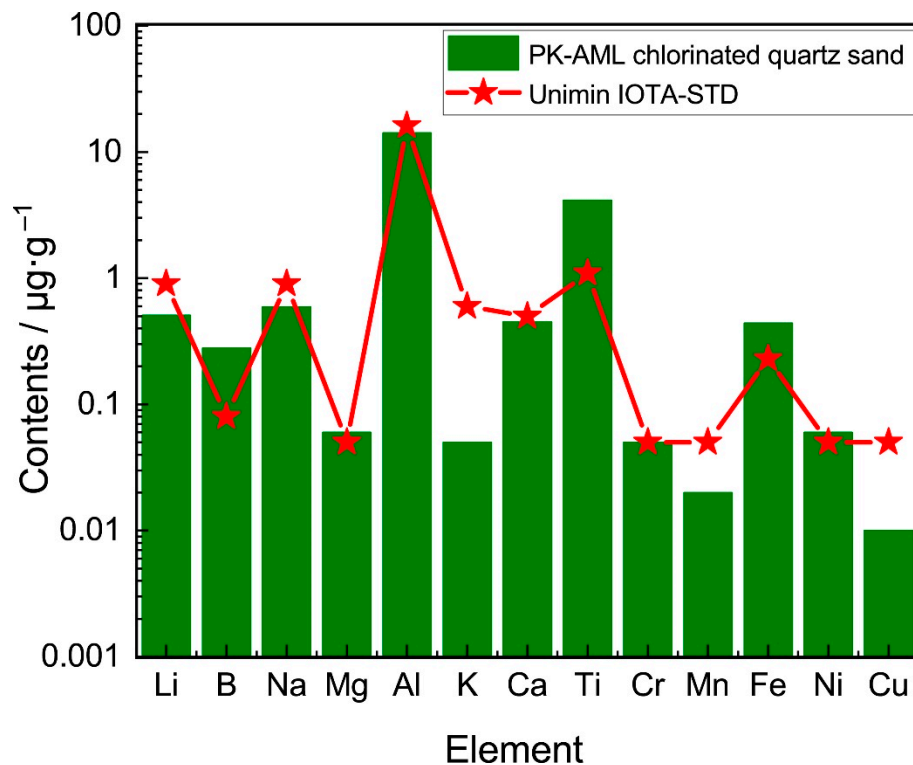

Figure 8. Thirteen main impurity elements in PK-AML chlorinated quartz sand compared with Unimin standard sand.

The semiconductor industry places the most stringent requirements on quartz purity. HPQ products are used in the semiconductor industry, such as quartz crucibles and crystalline silicon. From the growth of single-crystal silicon in quartz crucibles to the subsequent processing of wafers in clean rooms, HPQ crucible ware is employed. The high purity of the quartz prevents the contamination of wafers during the different processing steps [39]. According to earlier research and comprehensive analyses of relevant standard data of crucibles prepared by previous enterprises, it was found that the six key impurity elements that affect the application performance of HPQ are Al, Ti, Ca, K, Na, and Li, and their content requirements are Al < 14 $\mu g \cdot g^{-1}$, Ti < 4 $\mu g \cdot g^{-1}$, Ca < 2 $\mu g \cdot g^{-1}$, K < 1 $\mu g \cdot g^{-1}$, Na < 1 $\mu g \cdot g^{-1}$, and Li < 1 $\mu g \cdot g^{-1}$, respectively [37]. Therefore, the content of these six key impurity elements in the PK-AML processed quartz sand prepared in this study meets the requirements related to the preparation of crucibles by industries, indicating that PK-AML vein quartz can be used for the preparation of high-end HPQ products. However, the SiO_2 content of PK-JTLT quartz is relatively low, and it is difficult to remove high levels of impurity elements such as Li, Al, and Ti through purification experiments. This limitation restricts its application in high-end HPQ products. According to the specification requirements of photovoltaic glass ($SiO_2 \geq 99.95\%$), PK-JTLT quartz after experimental purification exceeds the industrial standards set for photovoltaic glass. It also exceeds the

industrial standards for electronic glass, optical glass, and support glass. Therefore, it is recommended for use as a raw material in the production of photovoltaic glass, electronic glass, optical glass, and other high-quality glass industries, indicating broad potential for future applications.

6. Conclusions

The present study investigates the gangue minerals, microstructures, and inclusion characteristics of the two vein quartz samples from Pakistan using optical microscopy, Raman spectroscopy, and scanning electron microscopy (SEM). Various purification processes were employed to evaluate the quality of the two vein quartz samples, aiming to achieve 4N8 HPQ. The specific conclusions are as follows:

(1) The quartz content of the PK-AML and PK-JTLT raw ore is high. The inclusions in PK-AML vein quartz are mainly secondary fluid inclusions arranged in a directional–linear manner or developed along crystal micro-cracks, with some areas of the crystal being clean, indicating that this vein quartz is a better quartz raw ore material. The PK-JTLT vein quartz contains a certain number of melt inclusions, which affects the quality of quartz.

(2) Flotation is a very important purification experiment for removing surface impurities and gangue minerals in vein quartz.

(3) Quartz sand calcination is superior to ore calcination. For quartz raw ore crushed into sand, the particles become finer and the specific surface area increases, which can more extensively expose the inclusions and lattice impurity elements within the quartz, making it more effective for subsequent acid leaching to remove impurities.

(4) The SiO_2 content of PK-AML processed quartz sand is 99.998 wt.% (4N8), meeting the relevant requirements of industries for the preparation of crucibles. The SiO_2 content of PK-JTLT processed quartz sand is 99.991 wt.%, meeting the relevant requirements of industries that use photovoltaic glass.

Author Contributions: Investigation, methodology and writing—original draft preparation, Y.X.; project administration and data curation, I.K. and Z.H.; resources, writing—review and editing, M.X. and X.Y. All authors have read and agreed to the published version of the manuscript.

Data Availability Statement: The data presented in this study are available in article.

Conflicts of Interest: The authors declared that they have no conflicts of interest to this work. We declare that we do not have any commercial or associative interest that represents a conflict of interest in connection with the work submitted.

References

1. Götze, J. Chemistry, textures and physical properties of quartz—Geological interpretation and technical application. *Min. Alogical Mag.* **2009**, *73*, 645–671. [CrossRef]
2. Rösler, H.J. *Lehrbuch der Mineralogie*, 2nd, ed.; VEB Deutscher Verlag für Grundstoffindustrie: Leipzig, Germany, 1981; Volume 833.
3. Li, X.L.; Zhang, Q.D.; Xu, H.X. Research on purification of quartz sand in Sichun. *Conserv. Util. Miner. Resour.* **2014**, *2*, 35–38. (In Chinese with English Abstract)
4. Englert, A.H.; Rodrigues, R.T.; Rubio, J. Dissolved air flotation (DAF) of fine quartz particles using an amine as collector. *Int. J. Miner. Process.* **2009**, *90*, 27–34. [CrossRef]
5. Haus, R. High demands on high purity. *Ind. Miner.* **2005**, *10*, 62–67.
6. Haus, R.; Prinz, S.; Priess, C. Assessment of High Purity Quartz Resources. In *Quartz: Deposits, Mineralogy and Analytics*; Springer: Berlin/Heidelberg, Germany, 2012; pp. 29–51.

7. Müller, A.; Ihlen, P.M.; Wanvik, J.E.; Flem, B. High-purity quartz mineralisation in kyanite quartzites, Norway. *Miner. Depos.* **2007**, *42*, 523–535. [CrossRef]

8. Shen, S.F. The actuality of study and manufacture in higher purity quartz. China Non-Met. *Min. Ind. Her.* **2006**, *5*, 13–16. (In Chinese with English Abstract)

9. Moore, P. High-purity quartz. *Ind. Miner.* **2005**, *455*, 53–57.

10. Yin, W.; Wang, D.; Drelich, J.W.; Yang, B.; Li, D.; Zhu, Z.; Yao, J. Reverse flotation separation of hematite from quartz assisted with magnetic seeding aggregation. *Miner. Eng.* **2019**, *139*, 105873. [CrossRef]

11. Rohem Peçanha, E.; da Fonseca de Albuquerque, M.D.; Antoun Simao, R.; de Salles Leal Filho, L.; de Mello Monte, M.B. Interaction forces between colloidal starch and quartz and hematite particles in mineral flotation. *Colloids Surf. A Physicochem. Eng. Asp.* **2019**, *562*, 79–85. [CrossRef]

12. Yang, L.; Li, W.; Li, X.; Yan, X.; Zhang, H. Effect of the turbulent flow pattern on the interaction between dodecylamine and quartz. *Appl. Surf. Sci.* **2020**, *507*, 145012. [CrossRef]

13. Khalifa, M.; Ouertani, R.; Hajji, M.; Ezzaouia, H. Innovative technology for the production of high-purity sand silica by thermal treatment and acid leaching process. *Hydrometallurgy* **2019**, *185*, 204–209. [CrossRef]

14. Shaban, M.; Abukhadra, M.R. Enhancing the Technical Qualifications of Egyptian White Sand Using Acid Leaching; Response Surface Analysis and Optimization. *Int. J. Miner. Process. Extr. Metall.* **2016**, *1*, 33–40.

15. Lin, M.; Lei, S.; Pei, Z.; Liu, Y.; Xia, Z.; Xie, F. Application of hydrometallurgy techniques in quartz processing and purification: A review. *Metall. Res. Technol.* **2018**, *115*, 303. [CrossRef]

16. Zhang, Q.D.; Li, X.L.; Song, Y.S.; Zhou, G.Y. Experimental Research on Preparation Technics of High-Purity Quartz Material. *Key Eng. Mater.* **2017**, *748*, 17–21. [CrossRef]

17. Buttress, A.J.; Rodriguez, J.M.; Ure, A.; Ferrari, R.S.; Dodds, C.; Kingman, S.W. Production of high purity silica by microflu-idic-inclusion fracture using microwave pretreatment. *Miner. Eng.* **2019**, *131*, 407–419. [CrossRef]

18. Li, F.; Jiang, X.; Zuo, Q.; Li, J.; Ban, B.; Chen, J. Purification mechanism of quartz sand by combination of microwave heating and ultrasound assisted acid leaching treatment. *Silicon* **2021**, *13*, 531–541. [CrossRef]

19. Wang, L. The concept of high purity quartz and the classification of raw materials. *Conserv. Util. Miner. Resour.* **2022**, *5*, 55–63.

20. Götze, J. Mineralogy, geochemistry and cathodoluminescence of authigenic quartz from different sedimentary rocks. In *Quartz: Deposits, Mineralogy and Analytics*; Götze, J., Möckel, R., Eds.; Springer: Berlin/Heidelberg, Germany, 2012; pp. 287–306.

21. Yang, X.Y.; Sun, C.; Cao, J.Y.; Shi, J.B. Research progress and development trend of high purity quartz. *Earth Sci.* **2021**, *29*, 231–244.

22. Wang, L.; Dang, C.P.; Li, C.X. Technology of high-purity quartz in China: Status quo and prospect. *Earth Sci. Front.* **2014**, *21*, 267–273.

23. Wang, L. Industrial types and application characteristics of quartz ore deposits. *Conserv. Util. Miner. Resour.* **2019**, *39*, 39–47.

24. Zhong, L.L. Study on Purifying Preparation and Mechanism. Master's Thesis, Wuhan University of Technology, Wuhan, China, 2015.

25. Zhang, D.H. Experimental Study on Processing 5N High Purity Quartz with Vein Quartz as Raw Material. Master's Thesis, Chengdu University of Technology, Chengdu, China, 2016.

26. Zhong, T.; Yu, W.; Shen, C.; Wu, X. Research on Preparation and Characterisation of High-purity Silica Sands by Purification of Quartz Vein Ore from Dabie Mountain. *Silicon* **2021**, *14*, 4723–4729. [CrossRef]

27. Li, Y.A. Study on Chemical Purification Method for Preparation of High Purity Quartz Sand from Vein Quartz. Master's Thesis, Southwest University of Science and Technology, Mianyang, China, 2013.

28. Wu, X. Study on Raw Material Selection Evaluation and Purification Technology of High Purity Quartz. Master's Thesis, Southwest University of Science and Technology, Mianyang, China, 2013.

29. Lin, M.; Pei, Z.Y.; Lei, S.M. Mineralogy and processing of hydrothermal vein quartz from hengche, Hubei Province (China). *Minerals* **2017**, *7*, 161. [CrossRef]

30. Zhu, Y.B.; Peng, Y.J.; Gao, H.M. Research on mineral processing of coastal quartz sand mine. *J. Wuhan Polytech. Univ.* **1999**, *21*, 37–39.

31. Zhao, H.L. Experimental study on iron removal from quartz sand by ultrasonic wave. *Glass Enamel* **2004**, *23*, 44–49.

32. Larsen, E.; Kleiv, R.A. Flotation of quartz from quartz-feldspar mixtures by the HF method. *Miner. Eng.* **2016**, *98*, 49–51. [CrossRef]

33. Crundwell, F.K. On the mechanism of the flotation of oxides and silicates. *Miner. Eng.* **2016**, *95*, 185–196. [CrossRef]

34. Jiang, X.S.; Chen, J.; Ban, B.Y.; Song, W.F.; Chen, C.; Yang, X.Y. Application of competitive adsorption of ethylenediamine and polyetheramine in direct float of quartz from quartz feldspar mixed minerals under neutral pH conditions. *Miner. Eng.* **2022**, *188*, 107850. [CrossRef]

35. Jiang, X.S.; Chen, J.; Wei, M.N.; Li, F.F.; Ban, B.Y.; Li, J.W. Effect of impurity content difference between quartz particles on flotation behavior and its mechanism. *Powder Technol.* **2020**, *375*, 504–512. [CrossRef]

36. Xu, L.; Tian, J.; Wu, H.; Lu, Z.; Sun, W.; Hu, Y. The flotation and adsorption of mixed collectors on oxide and silicate minerals. *Adv. Colloid Interface Sci.* **2017**, *250*, 1–14. [CrossRef]

37. Zhang, H.Q.; Tan, X.M.; Ma, Y.M.; Chen, C.L.; Zhang, S.H.; Wang, L.; Liu, L.; Zhu, L.K.; Guo, L.X.; Zhang, H.L.; et al. Geological characteristics and 4N8 grade product preparation technology of Altai pegmatite type high purity quartz deposit in Xinjiang. *Conserv. Util. Miner. Resour.* **2022**, *5*, 1–7.

38. Zuo, Q.X.; Liu, J.W.; Chen, J. Study on deep purification and kinetics of Fengyang quartz sand by calcination, quenching and acid leaching. *Conserv. Util. Miner. Resour.* **2022**, *5*, 76–81.
39. Pan, X.D. Resource, characteristic, purification and application of quartz: A review. *Miner. Eng.* **2022**, *183*, 107600. [CrossRef]
40. Lou, C.L.; Zhang, G.J.; OuYang, B.H.; Liu, Z.L. Study on high temperature chlorination purification of quartz sand. *Ind. Miner. Process.* **2020**, *1*, 16–19.
41. Yang, D.B.; Dong, F.Y.; Han, T.; Wang, F.Y.; Hang, Y.Q. Investigation of the Kinetics of hot press leaching for low-grade vein quartz. *Non Met. Mines* **2024**, *47*, 70–72.
42. Fraser, J.E.; Searle, M.P.; Parrish, R.R.; Noble, S.R. Chronology of deformation, metamorphism, and magmatism in the southern Karakoram Mountains. *GSA Bull.* **2001**, *113*, 1443–1455. [CrossRef]
43. Crawford, M.B.; Searle, M.P. Collision-related granitoid magmatism and crustal structure of the Hunza Karakoram, North Pakistan. *Geol. Soc. Lond. Spec. Publ.* **1993**, *74*, 53. [CrossRef]
44. Crawford, M.B.; Windley, B.F. Leucogranites of the Himalaya/Karakoram: Implications for magmatic evolution within collisional belts and the study of collision-related leucogranite petrogenesis. *J. Volcanol. Geotherm. Res.* **1990**, *44*, 1–19. [CrossRef]
45. Searle, M.P. *Geology and Tectonics of the Karakoram Mountains*; John Wiley & Sons Incorporated: New York, NY, USA, 1991.
46. Le Fort, P.; Michard, A.; Sonet, J.; Zimmermann, J. *Granites of Himalayas, Karakoram and Hindu Kush*; Institute of Geology, Punjab University: Lahore, Pakistan, 1983; pp. 235–255.
47. Musée National d'histoire Naturelle. Available online: https://www.mnhn.lu/from-dark-to-light-exhibition-texts/exceptional-deposits/the-pegmatites-of-karakorum-in-pakistan/ (accessed on 20 September 2024).
48. Malkani, M.S. Mineral Resources of Gilgit Baltistan and Azad Kashmir, Pakistan: An Update. *Open J. Geol.* **2020**, *10*, 661–702. [CrossRef]
49. Ning, S.Y.; Pan, B.K.; Chen, Y.G.; Chen, H.R.; Zhang, Z.Y. Microstructure and inclusions characteristics of vein quartz in Yangjiang area, Guangdong. *China Non Met. Miner. Ind.* **2020**, *5*, 65–68.
50. Xia, M.; Yang, X.Y.; Hou, Z.H. Preparation of High-Purity Quartz Sand by Vein Quartz Purification and Characteristics: A Case Study of Pakistan Vein Quartz. *Minerals* **2024**, *14*, 727. [CrossRef]
51. Müller, A.; Wanvik, J.E.; Ihlen, P.M. Petrological and Chemical Characterisation of High-Purity Quartz Deposits with Examples from Norway. In *Quartz: Deposits, Mineralogy and Analytics*; Springer: Berlin/Heidelberg, Germany, 2012; pp. 71–118.
52. Roedder, E. Fluid Inclusions. In *Reviews in Mineralogy*; Mineralogical Society of America: Chantilly, VA, USA, 1984; Volume 12, 644p.
53. Al-maghrabi, N.H. Improvement of low-grade silica sand deposits in Jeddah Area. *J. King Abdulaziz Univ. Eng. Sci.* **2004**, *15*, 113–128. [CrossRef]
54. Pang, Q.L.; Shen, J.X.; Cheng, C.B.; Guo, H.C.; Sun, X.; Li, W. Processing technology and application of high purity quartz. *Jiangsu Ceram. Acad. Res.* **2020**, *53*, 43–46.
55. Demir, C.; Gülgonul, I.; Bentli, I.; Çelik, M. Differential separation of albite from microcline by monovalent salts in HF medium. *Min. Metall. Explor.* **2003**, *20*, 120–124. [CrossRef]
56. Crozier, R.D. Non-metallic mineral flotation. *Ind. Miner.* **1990**, *269*, 55–65.
57. Wang, L.; Sun, W.; Hu, Y.H.; Xu, L.H. Adsorption mechanism of mixed anionic/cationic collectors in Muscovite—Quartz flotation system. *Miner. Eng.* **2014**, *64*, 44–50. [CrossRef]
58. Brant, J.A.; Johnson, K.M.; Childress, A.E. Examining the electrochemical properties of a nanofiltration membrane with atomic force microscopy. *J. Membr. Sci.* **2006**, *276*, 286–294. [CrossRef]
59. Liu, J.W. Study on Purification of Silica Sand by Roasting and Acid Leaching. Master's Thesis, Anhui University, Hefei, China, 2017.
60. Zhao, Z.K.; Sun, Q.Z.; Zhang, P.Q.; Jing, H.O.; Sun, Y.M. Effect of high temperature roasting on the surface of quartz sand. *Acta Mineral. Sin.* **2005**, *25*, 385–388.
61. Pan, J.L. Experimental Study on Preparation of 4N8 Standard High Purity Quartz by Chlorination Roasting. Master's Thesis, Chengdu University of Technology, Chengdu, China, 2015.
62. Mao, L.W.; Gu, C.H.; Wu, J.X. Experimental study on production of high purity quartz sand by replacing crystal with vein quartz. *World Build. Mater.* **2010**, *31*, 1–4.